Vol. 30 (1999) ACTA PHYSICA POLONICA B No 6

TWO PHOTON PHYSICS AT A FUTURE LINEAR COLLIDER*

A. De Roeck

DESY, Notkestrasse 85, 22607 Hamburg, Germany

(Received April 5, 1999)

Physics opportunities in two photon collisions at a future linear collider are discussed. Several QCD related topics are described in detail.

PACS numbers: 13.60.–r

1. Introduction

Plans for the construction of a future high energy e^+e^- linear collider (LC) are being seriously considered since some time. Such a machine would be able to provide e^+e^- collisions at centre of mass system (CMS) energies in the range of 0.3–2 TeV, with luminosities in the range of 5–50 $\cdot 10^{33}$ cm$^{-2}s^{-1}$.

Apart from the very exciting electron-positron program (see *e.g.* [1]), such a facility offers the opportunity for a two-photon physics program at high energies, either by using the photons emitted from the lepton beams, which follow the well known WWA [2] energy dependence, or by using photon backscattering to construct a high energy photon linear collider (PLC). The former one gets basically for free with an e^+e^- collider, but the known disadvantage is the rapidly decreasing photon flux. For a PLC it is suggested [3] to use a high intensity laser beam to backscatter on the high energy electron beams of the linear collider. It allows to have a high luminosity of photons with about 70–80% of the electron beam energy. A plethora of measurements becomes accessible with a PLC, which are considered to be front line measurements: Higgs boson physics, top quark studies and searches for supersymmetric and composed particles. Additionally, several important studies related to QCD issues in 2-photon interactions, such as photon structure function measurements at lower x and higher Q^2 values than currently available become accessible. A photon collider is also a W

---

* Presented at the Cracow Epiphany Conference on Electron–Positron Colliders, Cracow, Poland, January 5–10, 1999.

factory. Couplings can be studied often in a complementary way compared to e^+e^- collisions, and the precision reached is competitive, if sufficiently high luminosities can be reached at a PLC.

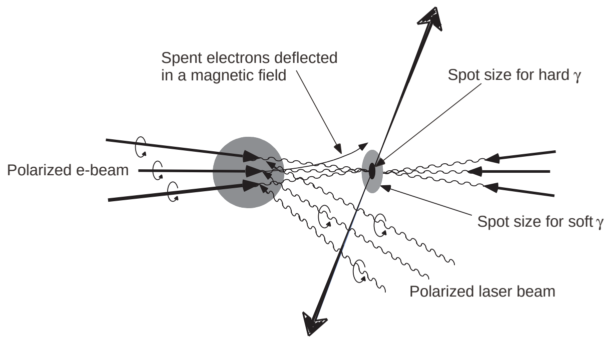

Fig. 1. A sketch of the creation of the photon beam by Compton backscattering of laser photons off the beam electrons, from Ref. [4].

The principle of the PLC is shown in Fig. 1: the high energy electron beam is converted into a high energy photon beam, by backscattering of photons of an intense laser beam, just before the interaction point. The maximum energy of the generated photons is given by $E_\gamma^{\max} = xE_e/(1+x)$, with E_e the electron beam energy and $x = 4E_eE_{\rm L}\cos^2(\theta/2)/m_e^2c^4$ with $E_{\rm L}$ and θ the laser photon energy and angle between the electron and laser beam. The distance of the conversion to the interaction point is in the range of several mm to a few cm. A typical value for x is 4.8, which leads to photon spectra which peak around $0.8E_e$, as shown in Fig. 2. The energy distribution depends on the polarisation of the photon (P_c) and electron beam (λ_e), as shown in Fig. 2: the most peaked spectrum is obtained when $P_c\lambda_e = -1$. The polarisation of the laser and electron beam can be further used to produce interactions with the same ($J_Z = 0$) or opposite ($J_Z = 2$) photon helicities, useful *e.g.* in Higgs studies.

If the Compton scattering is done only one side (two sides) then the collider produces eγ ($\gamma\gamma$) collisions. Note that a 2-photon collider would most likely use a e^-e^- collider as driver, rather than e^+e^- machine. For a $\gamma\gamma$ collider there will always be remaining eγ and e^+e^- luminosities, because some of the leftover electrons of the so called spent beams will reach the interaction region. These can be minimalized by tuning the optics, crab crossing angle or deflector magnets for the spent beam.

The critical parameters of a PLC are the achievable $\gamma\gamma$ luminosity, the energy spectrum of the Compton scattered photons, the resulting polarisation of the photon beam, the background produced at the interaction region, and the remaining eγ and e^-e^- luminosities.

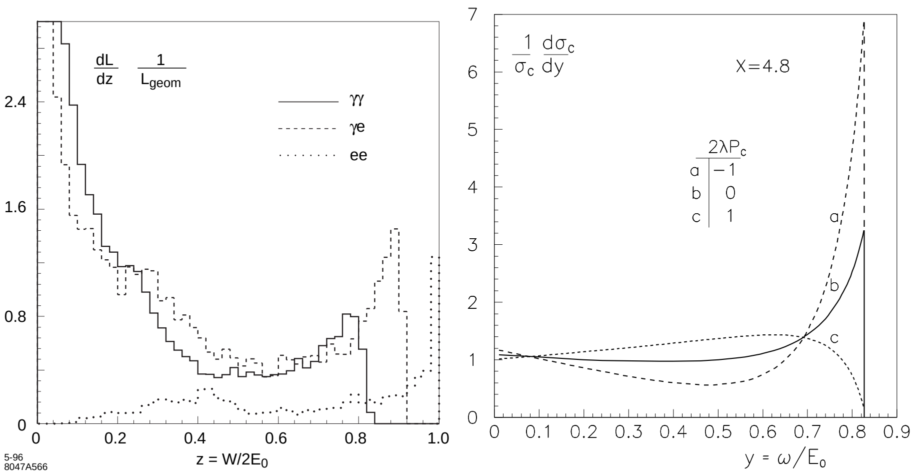

(a) (b)

Fig. 2. Some expected distributions for critical parameters of a PLC [4,6]. Shown are (a) the luminosity spectrum without deflection of the spent beam for a vertical offset of the beam of $0.75\sigma_y$ and a distance of between interaction and conversion point of 0.5 cm, (b) the energy spectrum of the Compton scattered photons for fixed x and different polarisations of the laser photons and the beam electrons as a function of the photon energy divided by the energy of the beam electrons.

The geometrical luminosity is given by $L_{\rm geom} = N^2 f/(4\pi\sigma_x\sigma_y)$, where N is the number of particles in the beam, f is the repetition frequency, and σ_x and σ_y are the transverse beam sizes at the interaction point. It has been argued [3] than higher geometrical luminosities can be achieved in e^+e^- colliders for photon colliders than for genuine e^+e^- colliders, due to the absence or strong reduction of beamstrahlung. In summary a typical distribution of $\gamma\gamma$ and $e\gamma$ luminosity as a function of the invariant mass peaks at the maximum reachable invariant mass of around $0.8\sqrt{s_{e^+e^-}}$ with widths of $\Delta W_{\gamma\gamma}/W_{\gamma\gamma} \approx 0.10 - 015$ for $\gamma\gamma$, and $\Delta W_{e\gamma}/W_{e\gamma} \approx 0.03 - 0.05$ for $e\gamma$ collisions [7]. The 'luminosity' is usually defined to be the luminosity corresponding to the region $0.65 < W_{\gamma\gamma} < W_{\gamma\gamma,\rm max}$ and is typically 10% of the geometrical luminosity $L_{\rm geom}$. Hence, with the luminosities as for TESLA [5], including a somewhat smaller horizontal β function at the interaction point, namely 2 mm, compared to the e^+e^- design, would lead to order 20 fb^{-1} event samples per year for the PLC.

The backgrounds in the interaction region of the LC are expected to be huge, due to beamstrahlung and pair production [8]. For the present version of TESLA [9] one expects about 150000 pairs per bunch crossing, depositing a total energy of 280 TeV. Most of these particles will go forward under

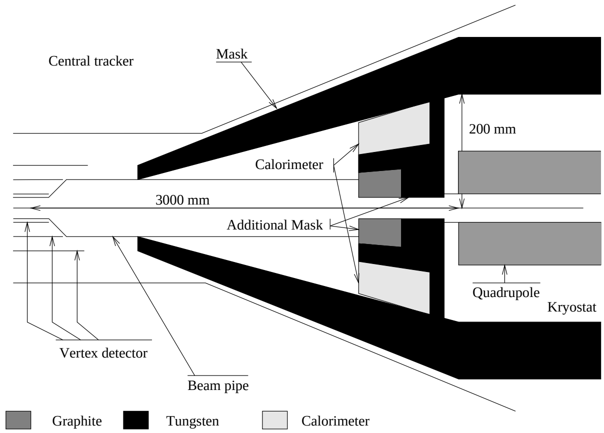

Fig. 3. A sketch of the proposed mask for the TESLA design to protect the detector from the background, from Ref. [8].

small angles, and remain in the beampipe. The deposited energy is several TeV for a θ_{min} above 10 mrad, and reduces further to a few hundred GeV for $\theta_{\rm min} > 20$ mrad, spread fairly uniformly in the azimuthal angle ϕ. As a result the detector has to be shielded with a massive mask, shown for the TESLA design in Fig. 3. Inside the mask however, it appears feasible to install electromagnetic calorimeters to tag scattered electrons in two-photon interactions in ee and $e\gamma$ collisions. The lowest angle to which these can be detected is presently thought to be 25 mrad.

2. Physics topics

2.1. Cross sections

First we discuss general PLC physics topics, and then we discuss specific QCD related topics which could be studied either at a photon collider or e^+e^- collider via the WWA photon spectrum. The cross sections for different reactions are compared in Fig. 4 for e^+e^-, $e\gamma$ and $\gamma\gamma$ reactions. One observes that the cross sections are generally larger in photon induced reactions. *e.g.* WW pair production at 500 GeV is a factor 20 larger than in e^+e^-. Even with the reduction of a factor $5-10$ of the luminosity compared to the corresponding e^+e^- machine, a $\gamma\gamma$ collider is a W factory with 10^6 WW-pairs for a PLC luminosity of 20 fb^{-1}. Cross sections for charged scalars, lepton and top pairs are a factor 5–10 higher at a PLC, compensating for the luminosity loss.

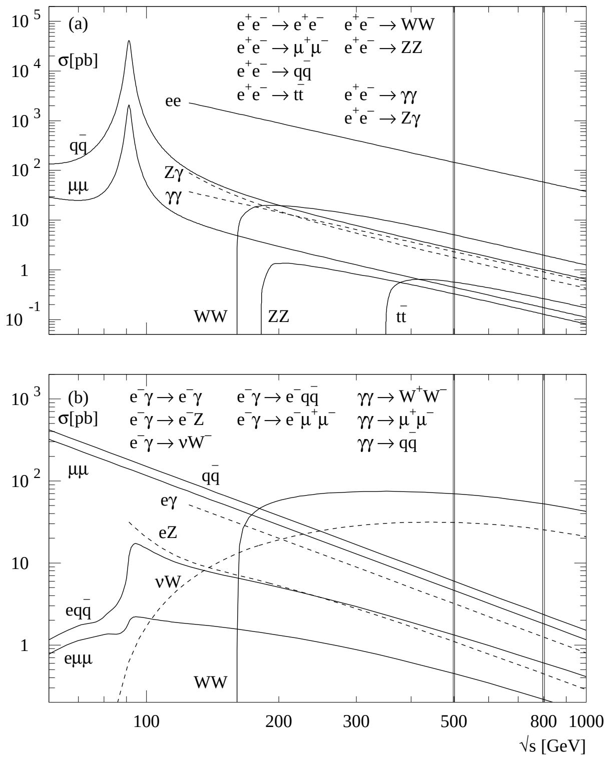

Fig. 4. The expected cross sections as a function of the centre-of mass energies, from Ref. [1]. Shown are (a) some e^+e^- reactions and (b) $e\gamma$ and $\gamma\gamma$ reactions, all as functions of the respective centre-of mass energy $\sqrt{s_{e^+e^-}}$, $\sqrt{s_{e\gamma}}$ or $\sqrt{s_{\gamma\gamma}}$.

2.2. Higgs bosons and supersymmetry

The quest for the Higgs particle(s) and the measurement of its properties will be one of the most important issues for high energy collider physics for the next years.

The PLC collider is an ideal place to search for the Higgs boson as at such a machine it is produced as an s-channel resonance. The mass reach of the PLC is up to 80% of the CMS of the e^-e^- collider.

For a light Higgs, the most promising channel is $\gamma\gamma \to H \to b\bar{b}$. Selecting $J_z = 0$ strongly suppresses the (Leading Order) contributions of $b\bar{b}$ and $c\bar{c}$ production, but a good tagging of bottom quarks with simultaneous rejection of charm quarks is needed. Thus the 2-photon decay width of the Higgs can be measured which is sensitive to all heavy charged particles, which acquire mass via the Higgs mechanism, and thus sensitive to new physics. An energy scan will allow a precise determination of the Higgs mass and width as well. A feasibility study has shown that the total width $\Gamma(H \to \gamma\gamma)$ can be determined with an $\mathcal{O}(10\%)$ error for an integrated luminosity of 10 fb^{-1} [10].

A potential of the search for supersymmetric particles at a PLC is evidenced in Fig. 5, where the selectron mass dependence is shown for different initial beam polarisations. It is noteworthy that the kinematic reach of the PLC (used in $e\gamma$ mode) is superior to the e^-e^+ machine.

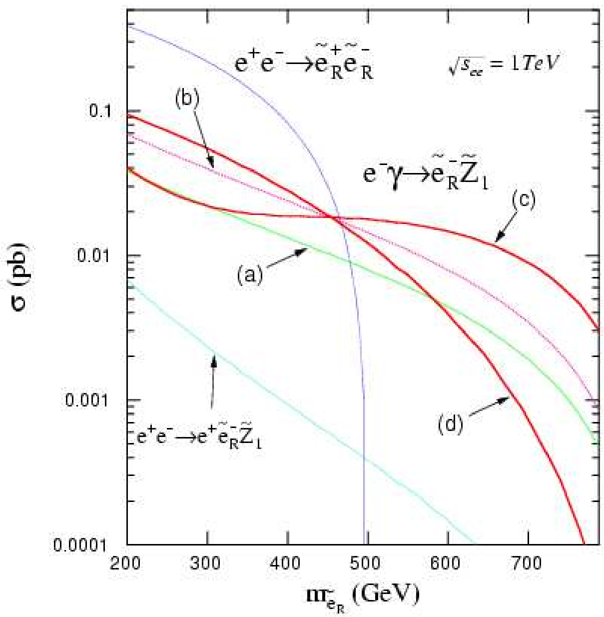

Fig. 5. Selectron mass dependence of the total cross section for each initial beam polarization $(\lambda_1, \lambda_2, P_c) = (0,0,0)$ (a), (+1/2,0,0,) (b), (+1/2,+1/2,-1) (c) and (+1/2,-1/2,+1) (d), for $\sqrt{s_{ee}} = 1$ TeV and $m_{\tilde{Z}_1} = 100$ GeV, from [11]

2.3. Total cross section and diffraction

At high $\gamma\gamma$ CMS energies $W_{\gamma\gamma}$ the total hadronic cross section $\sigma_{\gamma\gamma}$ for the production of hadrons in the interaction of two real photons is expected to be dominated by interactions where the photon has fluctuated into an hadronic state. Measuring the $W_{\gamma\gamma}$ dependence of $\sigma_{\gamma\gamma}$ should therefore improve our understanding of the hadronic nature of the photon and the universal high energy behaviour of total hadronic cross sections. New measurements at LEP show that the cross section rises at large $W_{\gamma\gamma}$, like for hadron–hadron and photon–hadron collisions as shown in Fig. 6. However the rise could be larger in $\gamma\gamma$ and measurements at the highest $W_{\gamma\gamma}$ are needed to establish this. In particular for the PLC mode measurements for $W_{\gamma\gamma}$ up to 400 GeV can be expected.

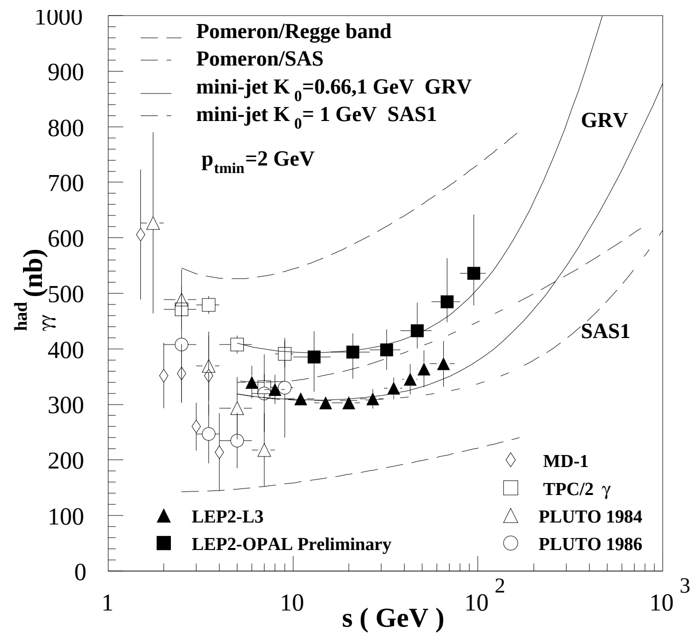

Fig. 6. The total cross section measurements and theoretical expectations. Shown are a comparison of the data with predictions from the eikonalised minijet model and Regge based models with extrapolations to higher energies, from Ref. [12].

Since $\gamma\gamma$ collisions act to a large extend as hadron–hadron collisions, diffractive components in the cross section are expected. The experimental acceptance for diffractive events is however rather small with present e^+e^- experiments, and needs an experimental check. Furthermore, diffraction is presently again a subject of high interest in high energy hadron–hadron and (virtual) photon-hadron interactions. Studies in photon–photon scattering can provide an important new field for high energy diffractive studies. One can benefit in particular from the varying beam energy and photon virtuality to further explore the nature of diffraction. Since soft processes cannot be calculated within perturbative QCD, it is difficult to obtain a reliable estimate for the expected cross section for photon diffraction dissociation, but about 20–30% of all $\gamma\gamma$ events are expected to belong to diffraction — either quasi-elastic vector meson production or diffraction dissociation.

Experimentally, events with diffraction dissociation can be identified using the rapidity gap technique. In non-diffractive reactions, rapidity gaps between the final state hadrons are exponentially suppressed. In contrast, the differential cross section $d\sigma_{\mathrm{SD},\gamma}/d\eta_{\mathrm{gap}}$ of diffraction dissociation at fixed

$W_{\gamma\gamma}$ is almost independent of the width η_{gap} of such rapidity gaps. Hence diffractive particle production can be measured triggering on large rapidity gaps.

As shown by the HERA Collaborations [15,16], the measurement of the so-called η_{max} distribution can be used to obtain experimental evidence for diffraction. The variable η_{max} is defined as the pseudorapidity of the most forward going hadron entering the central detector part, see Fig. 7.

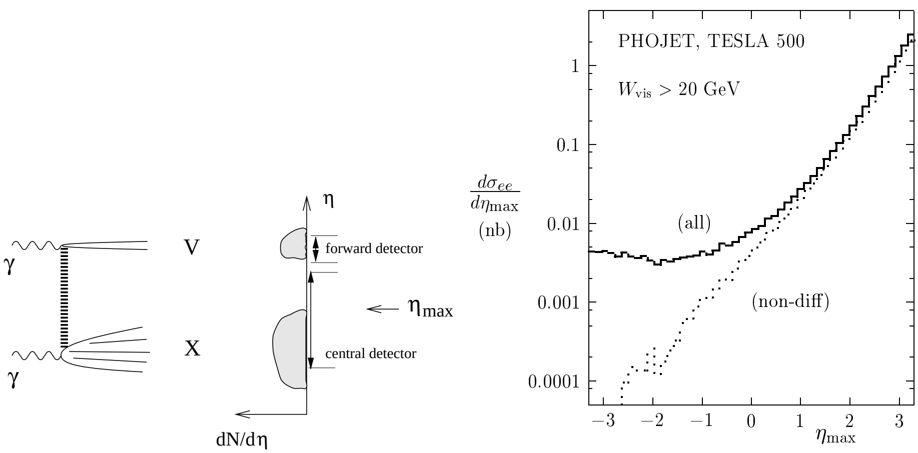

Fig. 7. (left) Photon single diffraction dissociation and the expected pseudorapidity distribution of final state hadrons. (right) The η_{max} cross section for the LC as calculated using the Phojet Monte Carlo event generator in two photon collisions with $W_{\mathrm{vis}} \geq 20$ GeV (full curve). The dotted curve shows the results of calculations for non-diffractive $\gamma\gamma$ interactions, from [17].

A prediction of the η_{max} cross section is shown in Fig. 7 for bremsstrahlung photon–photon interactions in e^+e^- collisions at a Linear Collider ($\sqrt{s}_{ee} = 500$ GeV). The η_{max} distribution is obtained using the hadrons produced at pseudorapidities in the central range $-3.3 \leq \eta \leq 3.3$. Only events having also particles produced in very forward direction ($3.5 \leq \eta \leq 4.0$) are accepted. A cut on the visible invariant mass $W_{\mathrm{vis}} > 20$ GeV was applied. The exponential suppression of the rapidity gap in non-diffractive events is clearly seen (dotted curve). A breakdown of the different components shows that for $W_{\mathrm{vis}} > 20$ GeV, the η_{max} region from -2 to -1 is clearly dominated by single diffraction dissociation of the photon along the $-z$ axis whereas for $\eta_{\mathrm{max}} < -2$ quasi-elastic vector meson production becomes important.

2.4. The structure of the photon

A photon may fluctuate into a bound or unbound quark–antiquark system and correspondingly develop a hadronic structure. This structure can be measured in certain reactions and then transported in calculations for cross sections in other collisions involving incoming photons. Traditional measurements are those of F_2^γ, as measured in $e\gamma$ interactions using the WWA photon spectrum in e^+e^- collisions. The latest results are from LEP and cover the Q^2 range from about 1.5 to 300 GeV^2 and the x range from 0.001 to about 1. The kinematics of the scattered electron and scattered quark out of the real photon for $e\gamma$ collisions with an electron of 250 GeV and a photon of 200 GeV is shown in Fig. 8. The detector acceptance for the scattered electrons is approx. $\theta_e = 25$ mrad and $E_e = 50$ GeV. This allows measurements in the region from $Q^2 > 10$ GeV^2 up to $Q^2 = 10^5$ GeV^2, and in x down to $x = 10^{-4}$. Will the F_2^γ start to show a strong rise with decreasing x as seen for the proton at HERA? The lower limit of 50 GeV for the scattered electron energy opens the possibility to measure for the first time the hadronic structure function $F_{\rm L}$ of the photon. Fig. 9 shows the structure function measurement, for 20 fb^{-1} with statistical and systematic errors, the latter taken to be the same as the statistical ones, but not less than 3%.

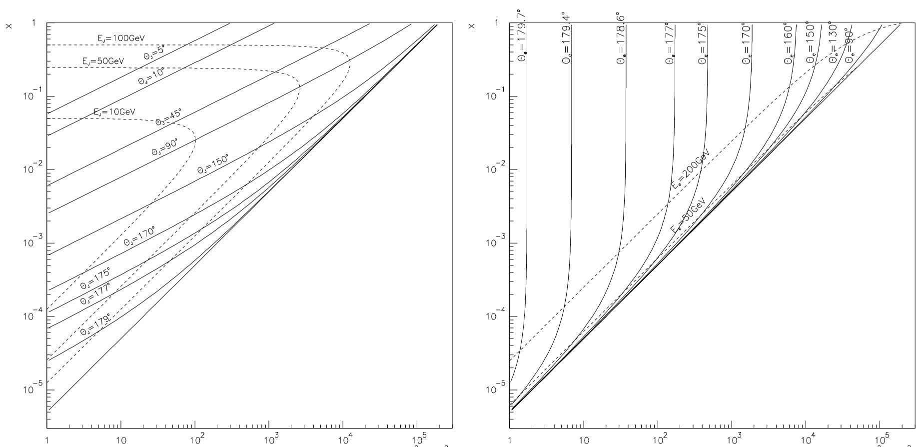

Fig. 8. The kinematics for 'Deep Inelastic' $e\gamma$ scattering at 250 GeV $\otimes$ 200 GeV at a future linear collider: (left) angles and energies for the current jet; (right) angles of the scattered electron. Angles are measured w.r.t. the photon direction.

Another important question for the LC data will be the Q^2 evolution of the structure function at medium x. The status of the present measurements is reviewed in Fig. 10, which is taken from Ref. [13] and extended

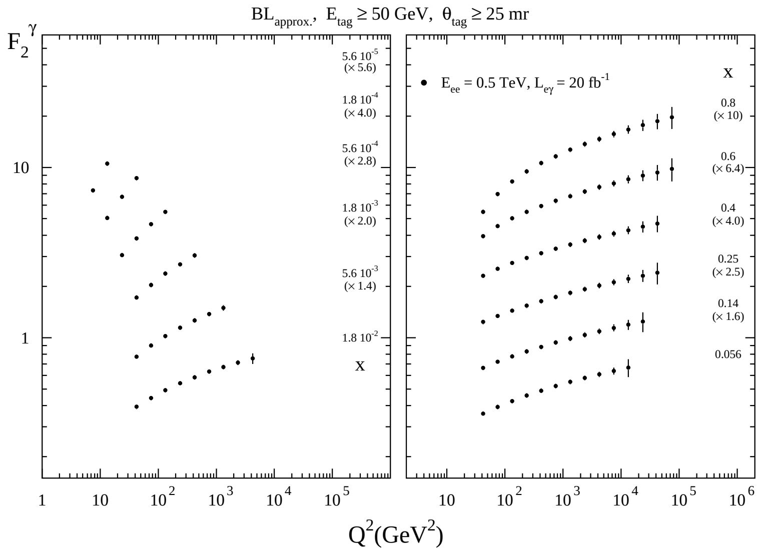

Fig. 9. The prospects for structure function measurements at a future linear collider. Shown are hypothetical linear collider data for a 25 mrad minimal detection angle of the scattered electrons, for 20 fb^{-1} at a PLC with 250 GeV electron beams, from [18].

by adding the preliminary measurement from L3 at $Q^2 = 120$ GeV^2. The prospects of the extension of the measurement at a future linear collider with $\sqrt{s} = 500$ GeVare shown for two scenarios in Fig. 10: one with minimal $\theta_{\rm tag} > 40$ mrad (LC1) and one with minimal $\theta_{\rm tag} > 175$ mrad (LC2). For both cases $E_{\rm tag}/E_b > 0.5$ is taken. These were the values considered for the '96 LC workshop [1]. The measured values are taken to be equal to the prediction of the leading order GRV [14] photon structure function in the respective ranges in x, which are chosen to be $0.1 < x < 0.6$ for LC1 and $0.3 < x < 0.8$ for LC2. The systematic error is assumed to be 6.7% and to be independent of Q^2 and dominates the errors apart from the highest Q^2 values. It is clear from Fig. 10 that overlap in Q^2 with the existing data can only be achieved if electron detection with $\theta_{\rm tag} > 40$ mrad is possible. For $\theta_{\rm tag} > 175$ mrad sufficient statistics is only available for Q^2 above around 1000 GeV^2.

Structure functions can be measured in *ee* collisions, like at LEP, using the WWA beam spectrum. However then the energy of the probed photon, or correspondingly, the value of x has to be reconstructed from the hadronic final state. Already at LEP this has been a major hazard and insufficient understanding in the modeling of the hadronic final states has been preventive for precision measurements. Improvements in this understanding can be ex-

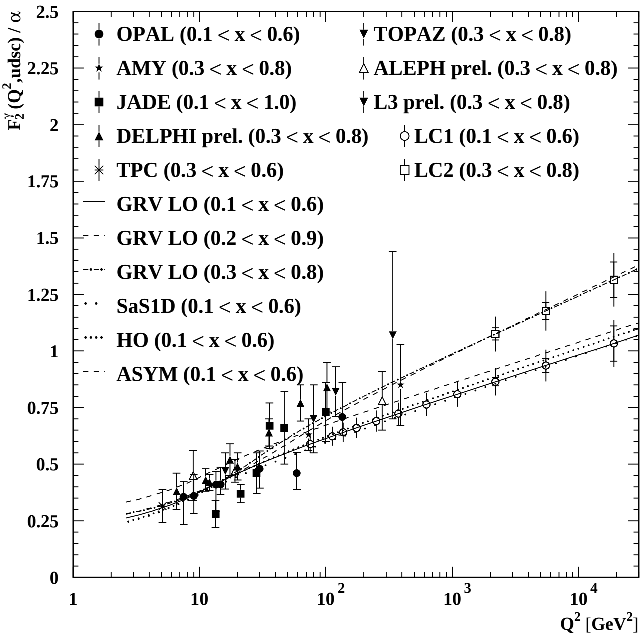

Fig. 10. The measured Q^2 evolution of the structure function from Ref. [13] extended by a preliminary measurement from L3 and by the prospects of a measurement at a future linear collider.

pected for the LC, however, due to the high collision energy poor acceptance of hadrons in the forward direction of the detectors, will make the task even more difficult for the LC data. The alternative is to tag the electron which emitted the (almost) real photon, and is correspondingly scattered under (almost) zero angle. Backgrounds make this non-trivial, and a case study is still ongoing. For a PLC a completely new avenue for photon structure function measurements would be opened. For the first time measurements could be performed with beams of high energetic photons of known energy with a rather small energy spread, a situation which starts to approach the one at HERA where the (proton) beam energy is exactly known.

2.5. Low-x physics

A QCD problem which has received as lot of attention both experimentally and theoretically in the last 10 years is the low-x regime. Fixed order perturbation theory is expected to fail in this region, where large logarithms $\sim \ln 1/x$ should show large contributions. In such a region resummation of the perturbation series to all orders is necessary. The BFKL equation performs such a resummation.

Several processes have recently been suggested for observing BFKL effect in high energy $\gamma\gamma$ collisions. Vector Meson production is discussed in [20]. Also forward jets has been studied [19] in $e\gamma$, an analogous process as currently being studied for ep collisions at HERA. The advantages of the linear collider are the potentially longer lever arm in x which could be reached and the more favourable kinematics to study 'forward physics' at the LC, as the $e\gamma$ collision produces the 'forward jets' more in the central detector.

A process to establish BFKL dynamics at e^+e^- interactions which is experimentally easier accessible is the total cross section of $\gamma^*\gamma^*$ scattering [21]. The measurement of this cross section requires the double tagging of both outgoing leptons in the forward direction. By varying the energy of the tagged leptons it is possible to probe the total cross section of the subprocess $\gamma^*\gamma^*$ from low energies up to almost the full energy of the e^+e^- collider. For sufficiently large photon virtualities we have a situation with only large momentum scales, similar to the 'forward jet measurement'. The energy dependence of this cross section, therefore, should be described by the power law of the BFKL pomeron.

A new calculation was proposed in [22], based on the dipole picture. The kinematic cuts used are as follows. "Perturbative" constraints are imposed by considering only photon virtualities Q_1^2, Q_2^2 high enough so that the scale μ^2 in α_S is greater than 3 GeV^2. To get valid perturbative BFKL calculations, $Y = \ln \hat{s}/\sqrt{Q_1^2 Q_2^2}$ is required to be larger than $\ln(\kappa)$ with $\kappa = 100$ in order to be in the high energy regime. Furthermore, in order to suppress DGLAP evolution, while maintaining BFKL evolution the constrain $0.5 < Q_1^2/Q_2^2 < 2.$ is used.

The results confirmed earlier findings on *e.g.* the strong dependence of the cross section on the minimum scattering angle of the tagged electrons. Table 1 and Fig. 11 give the results for a minimal angle of 40 mrad and one of 20 mrad. The effect of the energy of the tagged electron is also shown in Fig. 11. Hence it will be important to keep both the tagged angle and energy as low as possible. With 20 mrad the expected number of events from (LO) BFKL amounts to about 300000 for 100 fb^{-1}.

Recently it has been estimated that the higher order BFKL corrections can be very large. A phenomenological estimate of the effect has been made in [22], which assumes that the effective slope extracted with the dipole model from the inclusive F_2 and diffractive data at HERA can be transported to the $\gamma^*\gamma^*$ process. The result is shown in the third column of Table 1, and reveals that the strength of the effect, *i.e.* the comparison of the BFKL cross section with the one of the 2-gluons (absence of BFKL), is reduced by a factor 10. However the ratio of cross sections $\mathrm{BFKL_{HO}}$/2-gluons is still about 2.5.

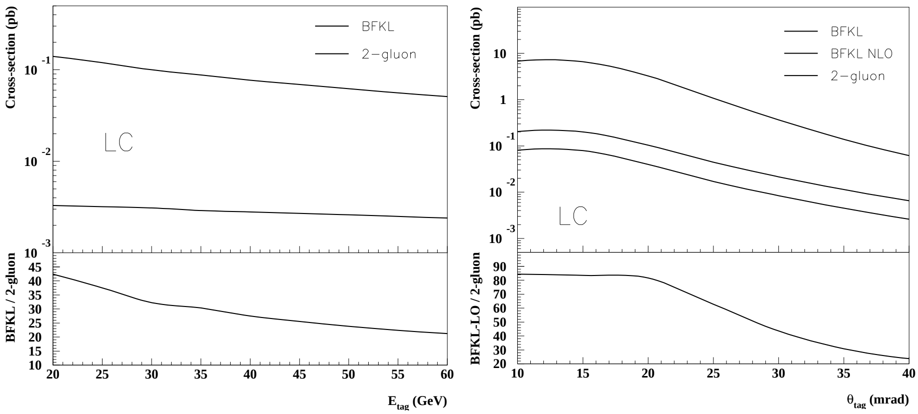

Fig. 11. Integrated BFKL and 2-gluon cross sections, at the LC. Leptons are tagged from $E_{\rm tag}$ up to the beam energy. We take $\theta_{\rm tag} > 40$ mrad at the LC. Integrated BFKL and 2-gluon cross sections at the LC, for various acceptances. Leptons are tagged between 50 and 250 GeV, from [22].

TABLE I

Final cross sections, for selections described in the text

	$BFKL_{\rm LO}$	$BFKL_{\rm HO}$	2-gluons	ratio
LC 40 mrad	6.2E-2	6.2E-3	2.64E-3	2.3
LC 20 mrad	3.3	0.11	3.97E-2	2.8

3. Conclusions

The prospects for 2-photon physics at a future linear collider facility are very large, in particular when a special interaction region using laser backscattering to produce photon beams becomes available. 2-photon physics can contribute to Higgs boson measurements, supersymmetric particle searches and push forward our QCD understanding of the structure of the photon and its hadronic interaction.

REFERENCES

[1] E. Accomando *et al.*, *Phys. Rep.* **299**, 1 (1998).

[2] C.F. Weizsäcker, *Z. Phys.* **88**, 612 (1934); E.J. Williams, *Phys. Rev.* **45**, 729 (1934).

[3] I.F. Ginzburg, G.L. Kotkin, V.G. Serbo, V.I. Telnov, *Nucl. Instrum. Methods Phys. Res.* **205**, 47 (1983); I.F. Ginzburg et al., *Nucl. Instrum. Methods Phys. Res.* **219**, 5 (1984); V. Telnov, *Nucl. Instrum. Methods Phys. Res.* **A294**, 72 (1990); V. Telnov, *Nucl. Instrum. Methods Phys. Res.* **A355**, 3 (1995).

[4] C. Adolphsen *et al.*, Zeroth-order design report for the Next Linear Collider, SLAC-474 (1996).

[5] R. Brinkmann *et al.*, Conceptual Design Report of a 500 GeV e^+e^- Linear Collider with Integrated X-ray Laser Facility, (1997).

[6] V. Telnov, High-energy photon-photon colliders, BUDKERINP-97-71, 18pp (1997), physics/9710014.

[7] V. Telnov, *Int. J. Mod. Phys.* **A13**, 2399 (1998); V. Telnov, KEK 98-163.

[8] D. Schulte, Study of electromagnetic and hadronic background in the interaction region of the TESLA collider, DESY-TESLA-97-08, 171pp (1997).

[9] D. Schulte, talk at the LC workshop in Frascati, November 1998.

[10] D.L. Borden, D.A. Bauer, D.O. Caldwell, *Phys. Rev.* **D48**, 4018 (1993).

[11] I. Watanabe *et al.*, KEK preprint 97-17.

[12] A. Corsetti, R.M. Godbole, G. Pancheri, *Phys. Lett.* **B435**, 441 (1998).

[13] R. Nisius, hep-ex/9712012, to be published. R. Nisius, hep-ex/9811024.

[14] M. Glück, E. Reya, A. Vogt, *Phys. Rev.* **D45**, 3986 (1992); M. Glück, E. Reya, A. Vogt, *Phys. Rev.* **D46**, 1973 (1992).

[15] ZEUS Collab. M. Derrick *et al.*, *Phys. Lett.* **B315**, 481 (1993).

[16] H1 Collab. T. Ahmed *et al.*, *Nucl. Phys.* **B429**, 477 (1994).

[17] A. De Roeck, R. Engel, A. Rostovtsev, hep-ph/9710366.

[18] A. Vogt, A. De Roeck, to be published.

[19] J.G. Contreras, A. De Roeck, to be published

[20] J. Kwieciński, L. Motyka, *Acta Phys. Pol.* **B30**, 1817 (1999).

[21] J. Bartels, A. De Roeck, H. Lotter, *Phys. Lett.* **B389**, 742 (1996); J. Bartels, A. De Roeck, C. Ewerz, H. Lotter, The $\gamma^\star\gamma^\star$ total cross section and the BFKL pomeron at the 500 GeV e^+e^- linear collider, (1997), hep-ph/9710500; S. Brodsky, F. Hautmann, D.E. Soper, *Phys. Rev.* **D56**, 6957 (1997); S. Brodsky, F. Hautmann, D.E. Soper, *Phys. Rev. Lett.* **78**, 803 (1997); Erratum, *Phys. Rev. Lett.* **79**, 3544 (1997).

[22] M. Boonekamp *et al.*, hep-ph/9812523.